IEEE Access
Multidisciplinary | Rapid Review | Open Access Journal

Received September 17, 2021, accepted October 1, 2021, date of publication October 4, 2021, date of current version October 12, 2021.

Digital Object Identifier 10.1109/ACCESS.2021.3117730

D-Type Iterative Learning Control for Open Container Motion System With Sloshing Constraints

GUANG LI[1], LI HOU[2], AND YONG LU[1,3]

[1]School of Information and Automation, Guangdong Polytechnic of Science and Trade, Guangzhou 510430, China
[2]School of Mechanical and Electrical Engineering, Guangdong Construction Polytechnic, Guangzhou 510440, China
[3]School of Automation Science and Engineering, South China University of Technology, Guangzhou 510641, China

Corresponding author: Guang Li (leeguang1028@163.com)

This work was supported in part by the Foundation for Young Innovative Talents in Higher Education of Guangdong under Grant 2018KQNCX410 and Grant 2021KQNCX183.

ABSTRACT In this paper, the iterative learning control (ILC) problem is investigated for the motion system of an open container with sloshing constraints in industrial fluid packaging. Initially, a broader class of second-order in space and first-order in time linear time-invariant singular distributed parameter system is decomposed by analyzing the motion system of an open container with sloshing constraints. Meanwhile, to eliminate the influence of singular terms on the system, a closed-loop D-type ILC algorithm is designed, and the corresponding convergence conditions are manifested. Then the convergence of the control algorithm is proved strictly. The resulting tracking error of systems can converge to any small tracking accuracy. Finally, a numerical example is given to verify the convergence and effectiveness of the closed-loop D-type ILC algorithm.

INDEX TERMS Sloshing constraints, iterative learning control, singular distributed parameter systems, convergence analysis.

I. INTRODUCTION

The fluid-filled container is stimulated by external excitations. It will facilitate the movement of the liquid inside the container. This movement of the free surface of the liquid is called liquid sloshing [1]. Liquid sloshing occurs widely in the fields of aerospace [2]–[4], industrial fluid packaging [5], [6], transportation [7]–[9], and so on. For example, the liquid in the fuel tank of the spacecraft will shake violently with the movement and attitude change of the spacecraft, which may lead to the attitude failure of the spacecraft and the failure of the fluid-filled container structure [10]. The liquid shaking in the fluid filling production line may cause the liquid in the tank to splash, contaminate the packaging seal, make the packaging seal lax, and affect the shelf life. The liquid filling production line is shown in Fig. 1. Therefore, the problem of liquid sloshing is getting more and more attention.

The associate editor coordinating the review of this manuscript and approving it for publication was Shun-Feng Su.

Liquid sloshing in a fluid-filled container is a relatively complex nonlinear dynamic system. At present, scholars have tried a lot of control methods for liquid sloshing. Among them, closed-loop control methods have made great development in the field of liquid sloshing suppression in liquid-filled containers, such as PID control [11], sliding mode control [12]–[15], and H-infinite control [16], [17]. The closed-loop controller takes the velocity or displacement change of the liquid-filled container as the input of the closed-loop system. In other control technologies, input signals are processed by filtering technology to generate predetermined input commands to achieve minimum sloshing targets, such as infinite impulse response filter [18], [19], acceleration compensation [20], and input shaping [21], [22], etc. In terms of the open-loop control of sloshing suppression, in [23], [24], the optimal path planning method is adopted to set the optimal motion trajectory with slight vibration. However, for more complex mechanical systems, it requires a large amount of computation to solve the inverse motion problem, which is not easy to achieve in engineering. In [25] adopts the digital filtering method. When the natural frequency of the mechanical system is in the low-pass filter band or the notch filter band, the digital filtering can effectively suppress the vibration of the mechanical system, but the robustness will become worse accordingly. In [26], the input shaping can effectively suppress the vibration of a single-mode system, but for a multi-mode mechanical system, because the high-order model is more complex and in the absence of relevant information, the inhibition effect of the Input Shaping is generalized.

Fluid motion within the liquid of the open container with sloshing constraints is described by the Navier-Stokes equations [27]. The model can be extended to the singular distributed parameter system (SDPS). Compared with the generalized system and the distributed parameter system [28], the singular distributed parameter system is more generally. When subjected to external disturbance, the system will not only lose its stability, but also change its structure significantly [29]. At the same time, the system has static and dynamic characteristics, so the control problem of the system has complexity [30]. At present, there are few theoretical achievements on singular distributed parameter systems, which mainly involve studying the properties of the system itself [31], [32] and the study on the control of the system as a controlled object [33]–[35].

Iterative learning control (ILC) is applied to a controlled system with repeated motion characteristics [28], and its goal is to complete the entire tracking task within a limited time interval [36]. It corrects the control signal according to the deviation between the output signal and the desired target, so as to improve the tracking performance of the system [28]. Iterative learning control is significant for nonlinear, strong coupling, difficult to model and repetitive motion of the controlled system [37], and it has been widely used in robot control, traffic flow control, industrial process, biomedical engineering and many other practical problems [38]–[43]. These practical problems have similar characteristics with the open container motion model with sloshing constraints, but the relevant research work is seldom reported at present. In this paper, the main innovations of iterative learning control for liquid sloshing model are as follows: (1) Different from the conventional method of controlling liquid sloshing, which includes PID control, sliding mode control, and H-infinite control, ILC is firstly applied to a class of SDPS generalized from the liquid sloshing model. For this class of nonlinear system, the ILC control effect is reasonable and effective, and the expected tracking error accuracy can be achieved; (2) This class of SDPS contains singular matrix coefficient terms, and the closed-loop D-type ILC algorithm is proposed to eliminate the influence of singular matrix for SDPS; (3) Through the rigor systematic research and analysis, sufficient conditions are presented to ensure that the tracking error of the liquid sloshing system is convergent by employing the definition of the $\mathbf{L}^2$ norm as well as some basic differential inequalities, and the strict mathematical proof of the convergence conditions are given. Finally, the numerical

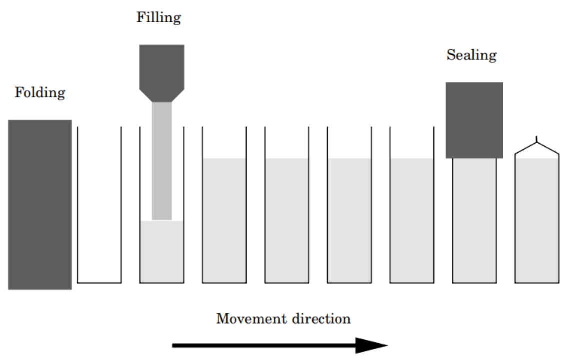

FIGURE 1. Schematic picture of the packaging machine.

simulation results are utilized to prove the effectiveness of the algorithm.

This paper includes the following structure. A broader class of SDPS generalized from the liquid sloshing model are controlled by the closed-loop D-type learning algorithm in Section II. Then the D-type learning algorithm is proposed, and the convergence condition is proved strictly in Section III. In Section IV, the D-type learning algorithm of SDPS is simulated. At last, in the conclusion section, the effectiveness of the D-type learning algorithm is illustrated.

Notations: The superscript 'T' represents the transpose of the matrix. $\mathbb{R}^{m\times n}$ represents the $m \times n$ real matrix, where $\mathbb{R}$ represents the set of real numbers. $A > 0$ represents a symmetric positive definite matrix and $A < 0$ means a negative definite matrix. If W is a matrix, the matrix norm of W is $\|W\| = \sqrt{\lambda_{max}(W^TW)}$. In another case, if we define $W = (w_1, w_2, \cdots, w_m)$ as a vector, then the Euclidean norm of W is $\|W\| = \sqrt{\sum_{i=1}^{m} W_i^2}$. $\lambda_{max}(\cdot)$ represents the maximum eigenvalue of W. If $x_i \in \mathbf{L}^2(\Omega)(i = 1, 2, \cdots, m)$ and let $x(z) = (x_1(z), x_2(z), \cdots, x_m(z)) \in \mathbb{R}^m \cap \mathbf{L}^2(\Omega)$, then $\|x\|_{\mathbf{L}^2} = \left\{\int_\Omega x(z)^T x(z)dz\right\}^{\frac{1}{2}}$. Let $f(z,t) : \Omega \times [0, T] \to \mathbb{R}^m$, $f(\cdot, t) \in \mathbb{R}^m \cap \mathbf{L}^2(\Omega)$, $\forall t \in [0, T]$, then $(\mathbf{L}^2, \lambda)$ norm of f is expressed as $\|f\|^2_{(\mathbf{L}^2,\lambda)} = \sup_{0\leqslant t\leqslant T}\left\{\|f(\cdot,t)\|^2_{\mathbf{L}^2} e^{-\lambda t}\right\}$.

II. SYSTEM DESCRIPTION AND PROBLEM FORMULATION

Fluid motion within the liquid is described by the so called Navier-Stokes equations [44] as follows:

$$\frac{\partial u}{\partial t} + (u \cdot \nabla)u + \nabla p - r\nabla^2 u = 0, \tag{1}$$

$$\nabla \cdot u = 0, \tag{2}$$

where $u = u(\xi, t)$ denotes a vector function, it is the velocity of the fluid, ξ is the position of the fluid particle. $p = p(\xi, t)$ is the pressure of the fluid particle, and ∇ denotes a spatial gradient operator, $r = \mu/\rho$ is called kinematic viscosity coefficient, μ is the first viscosity coefficient which is a constant, $\rho = \rho(\xi, t)$ is the density of the liquid. To illustrate the problem, only the expression form of the coefficient matrix in one dimension is given below. $x(u, p)$ is a marker, then the matrix form of the above system (1)-(2) can be described as follow:

$$\begin{pmatrix} 1 & 0 \\ 0 & 0 \end{pmatrix} \frac{\partial x}{\partial t} - r \begin{pmatrix} 1 & 0 \\ 0 & 0 \end{pmatrix} \frac{\partial^2 x}{\partial z^2} + \begin{pmatrix} u & 1 \\ 1 & 0 \end{pmatrix} \frac{\partial x}{\partial z} = 0. \tag{3}$$

Assuming the density of the liquid is constant, $r = \mu/\rho$ is a constant. The linearization system can be described as [45]:

$$\begin{pmatrix} 1 & 0 \\ 0 & 0 \end{pmatrix} \frac{\partial x}{\partial t} - r \begin{pmatrix} 1 & 0 \\ 0 & 0 \end{pmatrix} \frac{\partial^2 x}{\partial z^2} + \begin{pmatrix} \alpha & 1 \\ 1 & 0 \end{pmatrix} \frac{\partial x}{\partial z} = 0, \tag{4}$$

where α is the average velocity of a particle moving horizontally on the upper surface of the liquid. z is the position of the fluid particles moving in the horizontal direction. The linearized system belongs to a class of SDPS with parabolic. Based on the above application background [45], consider the following more general SDPS:

$$\begin{cases} E\dfrac{\partial x_k(z,t)}{\partial t} = D\dfrac{\partial^2 x_k(z,t)}{\partial z^2} + G\dfrac{\partial x_k(z,t)}{\partial z} \\ \qquad\qquad + Ax_k(z,t) + Bu_k(z,t), \\ y_k(z,t) = Cx_k(z,t). \end{cases} \tag{5}$$

where k denotes the number of iterations of the system (5). $t \in [0, T]$ represents the time index, T is a bounded positive number. $x_k(z,t) \in \mathbb{R}^m$, $y_k(z,t) \in \mathbb{R}^j$, $u_k(z,t) \in \mathbb{R}^n$ represent the system state, output and control input, respectively. In addition, $E \in \mathbb{R}^{m\times m}$ is the singular constant matrix, where $0 < rank(E) = r < m$. $D \in \mathbb{R}^{m\times m}$ is a diagonal positive definite constant matrix. $A \in \mathbb{R}^{m\times m}$, $B \in \mathbb{R}^{m\times n}$, $C \in \mathbb{R}^{j\times m}$ and $G \in \mathbb{R}^{m\times m}$ are constant matrices.

Remark 1: The liquid shaking in the fluid filling production line may cause the liquid in the container to splash, make the packaging seal lax, and affect the shelf life. Therefore, we must prevent the liquid from overflows the container. Let h is the limit height of the liquid in the container. We need to ensure that the liquid shaking level is below h, which means that the system output $y(z,t) < h$.

Before the ILC algorithm is given, the following assumptions would be useful in SDPS (5).

Assumption 1: For the desired output $y_d(z,t)$, there exists a desired input $u_d(z,t)$ such that

$$\begin{cases} E\dfrac{\partial x_d(z,t)}{\partial t} = D\dfrac{\partial^2 x_d(z,t)}{\partial z^2} + G\dfrac{\partial x_d(z,t)}{\partial z} \\ \qquad\qquad + Ax_d(z,t) + Bu_d(z,t), \\ y_d(z,t) = Cx_d(z,t). \end{cases} \tag{6}$$

Assumption 2: In the iteration learning process, the system (5) always satisfies the identical initial boundary conditions as follows,

$$\frac{\partial x_k(z,t)}{\partial z}|_{z=\partial\Omega} = 0, \quad (z,t) \in \partial\Omega \times [0,T],$$

$$x_k(0,t) = x_k(l,t) = 0, \quad t \in [0,T], \tag{7}$$

$$x_k(z,0) = \varphi(z) = x_d(z,0), \quad z \in \Omega,\ k = 1,2,3,\ldots \tag{8}$$

where $\Omega = [0, l]$, $\varphi(z)$ is a continuous function related to the spatial variable z. By finding a suitable learning algorithm, so that the system output sequence $y_k(z,t)$ has good tracking performance,

$$\lim_{k\to\infty} y_k(z,t) = y_d(z,t), \quad z \in \Omega,\ t \in [0,T].$$

III. CONVERGENCE ANALYSIS

In this section, we consider the following closed-loop D-type ILC algorithm [46]:

$$u_k(z,t) = u_{k-1}(z,t) + \Gamma\frac{\partial e_k(z,t)}{\partial t} \tag{9}$$

where $e_k(z,t) = y_d(z,t) - y_k(z,t)$ is the tracking error at the $k-th$ iteration. Then one gets the following lemma and theorem.

Lemma 1: Consider the parabolic SDPS (5). If there a gain matrix Γ such that the matrix $(E + B\Gamma C)$ is nonsingular, meanwhile the matrix $\tilde{G}$ is a positive definite matrix. That means $\tilde{G}^T\tilde{G} > 0$. By the definition of $(\mathbf{L}^2, \lambda)$ norm [33] and let Assumptions 1 to 2 be satisfied, it becomes

$$\|\bar{x}_k\|^2_{(\mathbf{L}^2,\lambda)} \le \frac{g}{\lambda - a}\|\bar{u}_{k-1}\|^2_{(\mathbf{L}^2,\lambda)}, \tag{10}$$

where $a = \|\tilde{A}\|^2 + 2$, $g = \|\tilde{B}\|^2$, $\lambda > a$,

$$\tilde{A} = (E + B\Gamma C)^{-1}A,$$
$$\tilde{B} = (E + B\Gamma C)^{-1}B,$$
$$\tilde{G} = (E + B\Gamma C)^{-1}G.$$

Proof: Denote $\bar{x}_k(z,t) = x_d(z,t) - x_k(z,t)$ and $\bar{u}_k(z,t) = u_d(z,t) - u_k(z,t)$, combining with (9), one has

$$\begin{aligned} \bar{u}_k(z,t) &= \bar{u}_{k-1}(z,t) - (u_k(z,t) - u_{k-1}(z,t)) \\ &= \bar{u}_{k-1}(z,t) - \Gamma\frac{\partial e_k(z,t)}{\partial t} \\ &= \bar{u}_{k-1}(z,t) - \Gamma C\frac{\partial \bar{x}_k(z,t)}{\partial t}. \end{aligned} \tag{11}$$

It follows from (5) and (6) that

$$\begin{aligned} E\frac{\partial \bar{x}_k(z,t)}{\partial t} &= D\frac{\partial^2 \bar{x}_k(z,t)}{\partial z^2} + G\frac{\partial \bar{x}_k(z,t)}{\partial z} \\ &\quad + A\bar{x}_k(z,t) + B\bar{u}_k(z,t). \end{aligned} \tag{12}$$

Substituting (11) into the above expression yields

$$\begin{aligned} E\frac{\partial \bar{x}_k(z,t)}{\partial t} &= D\frac{\partial^2 \bar{x}_k(z,t)}{\partial z^2} + G\frac{\partial \bar{x}_k(z,t)}{\partial z} + A\bar{x}_k(z,t) \\ &\quad + B[\bar{u}_{k-1}(z,t) - \Gamma C\frac{\partial \bar{x}_k(z,t)}{\partial t}]. \end{aligned} \tag{13}$$

Further, one has

$$\begin{aligned} (E + B\Gamma C)\frac{\partial \bar{x}_k(z,t)}{\partial t} &= D\frac{\partial^2 \bar{x}_k(z,t)}{\partial z^2} + G\frac{\partial \bar{x}_k(z,t)}{\partial z} \\ &\quad + A\bar{x}_k(z,t) + B\bar{u}_{k-1}(z,t). \end{aligned} \tag{14}$$

The matrix $(E + B\Gamma C)$ is nonsingular. So, one has

$$\begin{aligned} \frac{\partial \bar{x}_k(z,t)}{\partial t} &= \tilde{D}\frac{\partial^2 \bar{x}_k(z,t)}{\partial z^2} + \tilde{G}\frac{\partial \bar{x}_k(z,t)}{\partial z} \\ &\quad + \tilde{A}\bar{x}_k(z,t) + \tilde{B}\bar{u}_{k-1}(z,t), \end{aligned} \tag{15}$$

where

$$\tilde{D} = (E + B\Gamma C)^{-1}D$$
$$\tilde{G} = (E + B\Gamma C)^{-1}G$$
$$\tilde{A} = (E + B\Gamma C)^{-1}A$$
$$\tilde{B} = (E + B\Gamma C)^{-1}B.$$

Left multiplying both sides of (15) by $\bar{x}_k^T(z,t)$, one gets

$$\begin{aligned}\frac{1}{2}\frac{\partial[\bar{x}_k^T(z,t)\bar{x}_k(z,t)]}{\partial t} &= \bar{x}_k^T(z,t)\tilde{D}\frac{\partial^2\bar{x}_k(z,t)}{\partial z^2} \\ &+ \bar{x}_k^T(z,t)\tilde{G}\frac{\partial\bar{x}_k(z,t)}{\partial z} \\ &+ \bar{x}_k^T(z,t)\tilde{A}\bar{x}_k(z,t) \\ &+ \bar{x}_k^T(z,t)\tilde{B}\bar{u}_{k-1}(z,t). \end{aligned} \tag{16}$$

For Eq. (16) integrating about z on Ω, one gets

$$\begin{aligned}\frac{d}{dt}(\|\bar{x}_k(\cdot,t)\|_{\mathbf{L}^2}^2) &= 2\int_\Omega \bar{x}_k^T(z,t)\tilde{D}\frac{\partial^2\bar{x}_k(z,t)}{\partial z^2}dz \\ &+ 2\int_\Omega \bar{x}_k^T(z,t)\tilde{G}\frac{\partial\bar{x}_k(z,t)}{\partial z}dz \\ &+ 2\int_\Omega \bar{x}_k^T(z,t)\tilde{A}\bar{x}_k(z,t)dz \\ &+ 2\int_\Omega \bar{x}_k^T(z,t)\tilde{B}\bar{u}_{k-1}(z,t)dz \\ &\triangleq I_1 + I_2 + I_3 + I_4. \end{aligned} \tag{17}$$

Now, we will estimate $I_i, i = 1,2,3,4$. For I_1, it uses Green formula giving that,

$$\begin{aligned} I_1 &= 2\int_\Omega \bar{x}_k^T(z,t)\tilde{D}\frac{\partial^2\bar{x}_k(z,t)}{\partial z^2}dz \\ &= 2\int_\Omega \bar{x}_k^T(z,t)\tilde{D}d\frac{\partial\bar{x}_k(z,t)}{\partial z} \\ &= 2\frac{\partial\bar{x}_k^T(z,t)}{\partial z}\tilde{D}\bar{x}_k(z,t)\Big|_0^l \\ &\quad - 2\int_\Omega \frac{\partial\bar{x}_k^T(z,t)}{\partial z}\tilde{D}\frac{\partial\bar{x}_k(z,t)}{\partial z}dz. \end{aligned} \tag{18}$$

By employing the boundary conditions and $\tilde{D}^T\tilde{D} > 0$, one gets

$$I_1 \leq -2\lambda_{min}(\tilde{D}^T\tilde{D})\Big\|\frac{\bar{x}_k(\cdot,t)}{\partial z}\Big\|_{\mathbf{L}^2}^2 \leq 0. \tag{19}$$

For I_2, we use Green formula giving that,

$$\begin{aligned} I_2 &= 2\int_\Omega \bar{x}_k^T(z,t)\tilde{G}\frac{\partial\bar{x}_k(z,t)}{\partial z}dz \\ &= 2\int_\Omega \bar{x}_k^T(z,t)\tilde{G}d\bar{x}_k(z,t) \\ &= 2\bar{x}_k^T(z,t)\tilde{G}\bar{x}_k(z,t)\Big|_0^l \\ &\quad - 2\int_\Omega \bar{x}_k(z,t)\tilde{G}\bar{x}_k(z,t)dz. \end{aligned} \tag{20}$$

By employing the boundary conditions and $\tilde{G}^T\tilde{G} > 0$, one gets

$$I_2 \leq -2\lambda_{min}(\tilde{G}^T\tilde{G})\big\|\bar{x}_k(\cdot,t)\big\|_{\mathbf{L}^2}^2 \leq 0. \tag{21}$$

For I_3 and I_4, using Young's inequality, it leads to

$$\begin{aligned} I_3 &= 2\int_\Omega \bar{x}_k^T(z,t)\tilde{A}\bar{x}_k(z,t)dz \\ &\leq \|\tilde{A}\|^2\|\bar{x}_k(\cdot,t)\|_{\mathbf{L}^2}^2 + \|\bar{x}_k(\cdot,t)\|_{\mathbf{L}^2}^2, \end{aligned} \tag{22}$$

and

$$\begin{aligned} I_4 &= 2\int_\Omega \bar{x}_k^T(z,t)\tilde{B}\bar{u}_{k-1}(z,t)dz \\ &\leq \|\bar{x}_k(\cdot,t)\|_{\mathbf{L}^2}^2 + \|\tilde{B}\|^2\|\bar{u}_{k-1}(\cdot,t)\|_{\mathbf{L}^2}^2. \end{aligned} \tag{23}$$

Thus, from (19)-(23), one can obtain

$$\begin{aligned}\frac{d}{dt}(\|\bar{x}_k(\cdot,t)\|_{\mathbf{L}^2}^2) &\leq \|\tilde{A}\|^2\|\bar{x}_k(\cdot,t)\|_{\mathbf{L}^2}^2 + \|\bar{x}_k(\cdot,t)\|_{\mathbf{L}^2}^2 \\ &+ \|\bar{x}_k(\cdot,t)\|_{\mathbf{L}^2}^2 + \|\tilde{B}\|^2\|\bar{u}_{k-1}(\cdot,t)\|_{\mathbf{L}^2}^2 \\ &\leq a\|\bar{x}_k(\cdot,t)\|_{\mathbf{L}^2}^2 + g\|\bar{u}_{k-1}(\cdot,t)\|_{\mathbf{L}^2}^2, \end{aligned} \tag{24}$$

with $a = \|\tilde{A}\|^2 + 2$, $g = \|\tilde{B}\|^2$.

Inequality both sides of (24) about t, and applying the Bellman-Gronwall inequality, one has

$$\begin{aligned}\|\bar{x}_k(\cdot,t)\|_{\mathbf{L}^2}^2 \leq g\int_0^t &\|e^{a(t-s)}\bar{u}_{k-1}(\cdot,s)\|_{\mathbf{L}^2}^2 ds \\ &+ e^{at}\|\bar{x}_k(\cdot,0)\|_{\mathbf{L}^2}^2, \end{aligned} \tag{25}$$

Multiply both sides of the inequality (25) by $e^{-\lambda t}$, where $\lambda > a$, it gets

$$\begin{aligned} e^{-\lambda t}\|\bar{x}_k(\cdot,t)\|_{\mathbf{L}^2}^2 &\leq g\int_0^t e^{-(\lambda-a)(t-s)}\|\bar{u}_{k-1}(\cdot,s)\|_{\mathbf{L}^2}^2 e^{-\lambda s}ds \\ &+ e^{-(\lambda-a)t}\|\bar{x}_k(\cdot,0)\|_{\mathbf{L}^2}^2, \end{aligned} \tag{26}$$

Applying the definition of $(\mathbf{L}^2,\lambda)$ norm and known initial condition, we have

$$\|\bar{x}_k\|_{(\mathbf{L}^2,\lambda)}^2 \leq \frac{g}{\lambda - a}\|\bar{u}_{k-1}\|_{(\mathbf{L}^2,\lambda)}^2. \tag{27}$$

The proof of Lemma 1 is end.

Theorem 1: Let Assumptions 1 to 2 be satisfy. If there exists a gain matrix Γ such that $E + B\Gamma C$ is positive definite matrix and there exist an appropriate positive constant $\gamma > 0$ such that

$$2\gamma\|I - \Gamma C(E + B\Gamma C)^{-1}B\|^2 < 1. \tag{28}$$

Combine with the D-type learning algorithm (9), the system output $y_k(z,t)$ can track the desired trajectory, that is

$$\lim_{k\to\infty}\|e_k(\cdot,t)\|_{\mathbf{L}^2} = 0.$$

Proof: Substituting (15) into (11), one gets

$$\begin{aligned}\bar{u}_k(z,t) &= (I - \Gamma C\tilde{B})\bar{u}_{k-1}(z,t) - \Gamma C\tilde{A}\bar{x}_k(z,t) \\ &- \Gamma C\tilde{G}\frac{\partial\bar{x}_k(z,t)}{\partial z} - \Gamma C\tilde{D}\frac{\partial^2\bar{x}_k(z,t)}{\partial z^2}. \end{aligned} \tag{29}$$

Take integration about z from 0 to l, one gets

$$\begin{aligned}\int_0^l \bar{u}_k(z,t)dz = (I-\Gamma C\tilde{B})\int_0^l \bar{u}_{k-1}(z,t)dz\\ -\Gamma C\tilde{A}\int_0^l \bar{x}_k(z,t)dz\\ -\Gamma C\tilde{G}\int_0^l \frac{\partial \bar{x}_k(z,t)}{\partial z}dz\\ -\Gamma C\tilde{D}\int_0^l \frac{\partial^2 \bar{x}_k(z,t)}{\partial z^2}dz. \quad (30)\end{aligned}$$

Dealing with $\frac{\partial^2 \bar{x}_k(z,t)}{\partial z^2}$ and $\frac{\partial \bar{x}_k(z,t)}{\partial z}$by part integral, one has

$$\int_0^l \frac{\partial^2 \bar{x}_k(z,t)}{\partial z^2}dz = \left.\frac{\partial \bar{x}_k(z,t)}{\partial z}\right|_0^l = 0. \quad (31)$$

Then we have

$$\begin{aligned}\int_0^l \bar{u}_k(z,t)dz = (I-\Gamma C\tilde{B})\int_0^l \bar{u}_{k-1}(z,t)dz\\ -\Gamma C\tilde{A}\int_0^l \bar{x}_k(z,t)dz. \quad (32)\end{aligned}$$

Based on Eq. (32) and using Young's inequality, one gets

$$\begin{aligned}&\Big(\int_0^l \bar{u}_k(z,t)dz\Big)^T\Big(\int_0^l \bar{u}_k(z,t)dz\Big)\\ &\leq 2\Big(\int_0^l (I-\Gamma C\tilde{B})\bar{u}_{k-1}(z,t)dz\Big)^T\\ &\Big(\int_0^l (I-\Gamma C\tilde{B})\bar{u}_{k-1}(z,t)dz\Big)\\ &\quad +2\Big(\int_0^l \Gamma C\tilde{A}\bar{x}_k(z,t)dz\Big)^T\Big(\int_0^l \Gamma C\tilde{A}\bar{x}_k(z,t)dz\Big)\\ &\leq 2l\|I-\Gamma C\tilde{B}\|^2\|\bar{u}_{k-1}(\cdot,t)\|^2_{\mathbf{L}^2} + 2l\|\Gamma C\tilde{A}\|^2\|\bar{x}_k(\cdot,t)\|^2_{\mathbf{L}^2}. \quad (33)\end{aligned}$$

On the other hands, applying Jensen's inequality to the left side (33), one gets

$$\Big(\int_0^l \bar{u}_k(z,t)dz\Big)^T\Big(\int_0^l \bar{u}_k(z,t)dz\Big) \leq l\|\bar{u}_k(\cdot,t)\|^2_{\mathbf{L}^2}. \quad (34)$$

Then, there exist an appropriate positive constant $\gamma > 0$ such that,

$$\begin{aligned}\|\bar{u}_k(\cdot,t)\|^2_{\mathbf{L}^2} \leq 2\gamma\|I-\Gamma C\tilde{B}\|^2\|\bar{u}_{k-1}(\cdot,t)\|^2_{\mathbf{L}^2}\\ +2\gamma\|\Gamma C\tilde{A}\|^2\|\bar{x}_k(\cdot,t)\|^2_{\mathbf{L}^2}, \quad (35)\end{aligned}$$

Multiply both sides of Eq. (35) by $e^{-\lambda t}$ and applying the definition of $(\mathbf{L}^2,\lambda)$ norm gives

$$\begin{aligned}\|\bar{u}_k\|^2_{(\mathbf{L}^2,\lambda)} \leq 2\gamma\|I-\Gamma C\tilde{B}\|^2\|\bar{u}_{k-1}\|^2_{(\mathbf{L}^2,\lambda)}\\ +c_1\|\bar{x}_k\|^2_{(\mathbf{L}^2,\lambda)}, \quad (36)\end{aligned}$$

where $c_1 = 2\gamma\|\Gamma C\tilde{A}\|^2$. Through Lemma 1, substituting (27) into (36), one gives

$$\|\bar{u}_k\|^2_{(\mathbf{L}^2,\lambda)} \leq \Big[2\gamma\|I-\Gamma C\tilde{B}\|^2 + \frac{c_1 g}{\lambda - a}\Big]\|\bar{u}_{k-1}\|^2_{(\mathbf{L}^2,\lambda)}. \quad (37)$$

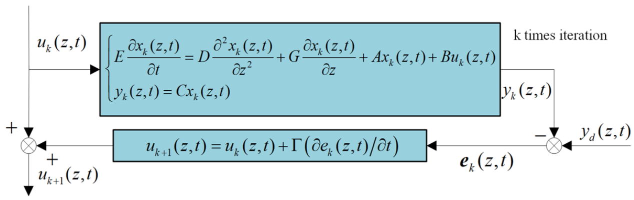

FIGURE 2. **D-type ILC algorithm control flow chart.**

According to the convergence conditions of Theorem 1, we have $2\gamma\|I-\Gamma C\tilde{B}\|^2 < 1$, we can find a and λ which sufficiently large to satisfy the following condition

$$2\gamma\|I-\Gamma C\tilde{B}\|^2 + \frac{c_1 g}{\lambda - a} < 1. \quad (38)$$

By the formulas (37) and (38), one gives

$$\lim_{k\to\infty}\|\bar{u}_k\|^2_{(\mathbf{L}^2,\lambda)} = 0, \quad (39)$$

which together with (27) yields

$$\lim_{k\to\infty}\|\bar{x}_k\|^2_{(\mathbf{L}^2,\lambda)} = 0. \quad (40)$$

Further, by employing (5) gives

$$\lim_{k\to\infty}\|e_k\|^2_{(\mathbf{L}^2,\lambda)} = \lim_{k\to\infty}\|C\|^2\|\bar{x}_k\|^2_{(\mathbf{L}^2,\lambda)} = 0. \quad (41)$$

Finally, by the following inequality

$$\begin{aligned}\|e_k(\cdot,t)\|^2_{\mathbf{L}^2} &= \big(\|e_k(\cdot,t)\|^2_{\mathbf{L}^2}\, e^{-\lambda t}\big)e^{\lambda t}\\ &\leq \|e_k\|^2_{(\mathbf{L}^2,\lambda)}e^{\lambda T}, \quad (42)\end{aligned}$$

which implies

$$\lim_{k\to\infty}\|e_k(\cdot,t)\|^2_{\mathbf{L}^2} = 0. \quad (43)$$

This completes the proof of Theorem 1.

IV. NUMERICAL SIMULATIONS

To illustrate the effectiveness of the closed-loop D-type ILC algorithm for SDPS constructed by slosh-constrained open container motion system in this paper, a specific numerical example is given as follows:

$$\begin{cases} E\dfrac{\partial x(z,t)}{\partial t} = D\dfrac{\partial^2 x(z,t)}{\partial z^2} + G\dfrac{\partial x(z,t)}{\partial z}\\ \qquad\qquad + Ax(z,t) + Bu(z,t),\\ y(z,t) = Cx(z,t). \end{cases} \quad (44)$$

where $(z,t) \in [0,1]\times[0,0.8]$, $x(z,t) \in \mathbb{R}^2$ represents the system status.

The coefficient matrix parameters are given as follows:

$$E = \begin{bmatrix}1 & 0\\ 0 & 0\end{bmatrix},\quad A = \begin{bmatrix}0.5 & 0\\ 0 & 0.2\end{bmatrix},\quad B = \begin{bmatrix}1 & 0\\ 0 & 2\end{bmatrix},$$
$$C = \begin{bmatrix}1 & 0\\ 0 & 1\end{bmatrix},\quad D = \begin{bmatrix}0.3 & 0\\ 0 & 0.2\end{bmatrix},\quad G = \begin{bmatrix}0.6 & 0\\ 0 & 0.25\end{bmatrix}.$$

The initial and boundary conditions are:

$$x_k(0,t) = x_k(1,t) = 0, \quad t \in [0,0.8],$$
$$x(z,0) = 0, \quad z \in [0,1].$$

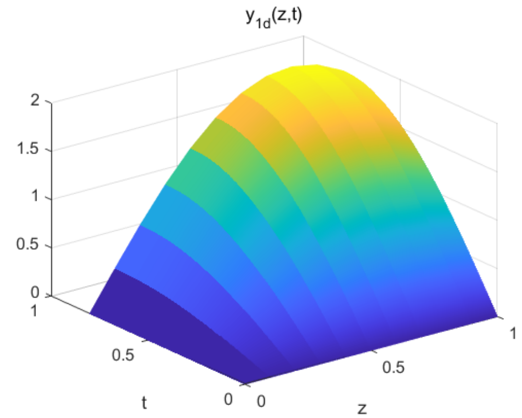

FIGURE 3. Desired surface $y_{1d}(z, t)$.

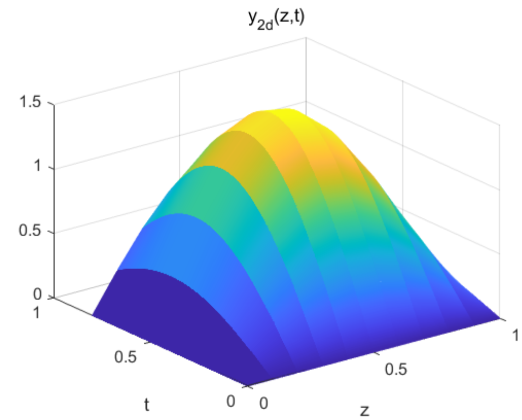

FIGURE 4. Desired surface $y_{2d}(z, t)$.

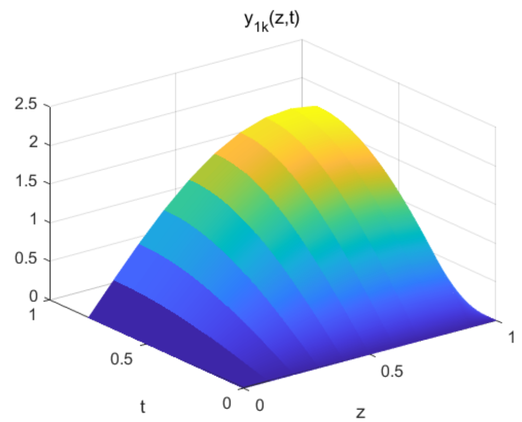

FIGURE 5. Actual output surface $y_{1k}(z, t)$ (k = 80).

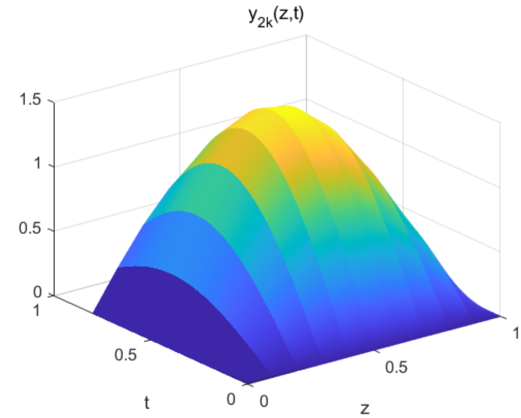

FIGURE 6. Actual output surface $y_{2k}(z, t)$ (k = 80).

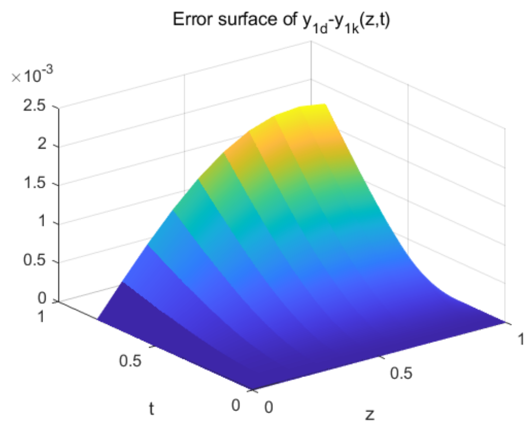

FIGURE 7. The output error surface of $y_{1d} - y_{1k}(z, t)$.

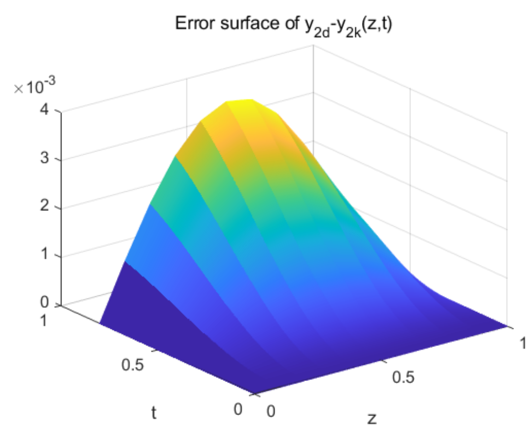

FIGURE 8. The output error surface of $y_{2d} - y_{2k}(z, t)$.

According to the D-type learning algorithm (9), the gain matrix is selected as $\Gamma = \begin{bmatrix} 0.5 & 0 \\ 0 & 0.2 \end{bmatrix}$. Then we have $E + B\Gamma C = \begin{bmatrix} 1.5 & 0 \\ 0 & 0.4 \end{bmatrix}, \tilde{G} = \begin{bmatrix} 0.4 & 0 \\ 0 & 0.625 \end{bmatrix}$, the matrix $\tilde{G}$ satisfies $\tilde{G}^T \tilde{G} > 0$. Furthermore, let $\gamma = 1$, we can compute that $\|I - \Gamma C(E + B\Gamma C)^{-1}B\|^2 < 0.5$. Then under the control of the learning algorithm (9), the output $y_k(z, t)$ of the system can uniformly converge to the desired trajectory.

The desired trajectory in space and time is given as:

$$\begin{bmatrix} y_{1d}(z, t) \\ y_{2d}(z, t) \end{bmatrix} = \begin{bmatrix} 2\sin(2t)\sin(2z) \\ 1.5\sin(3t)\sin(3z) \end{bmatrix},$$

with $(z, t) \in [0, 1] \times [0, 0.8]$.

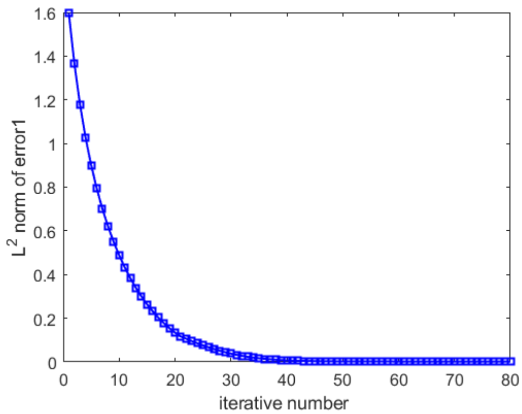

FIGURE 9. Maximum error $\|e_{1k}(\cdot,t)\|_{L^2}$-iteration number curve.

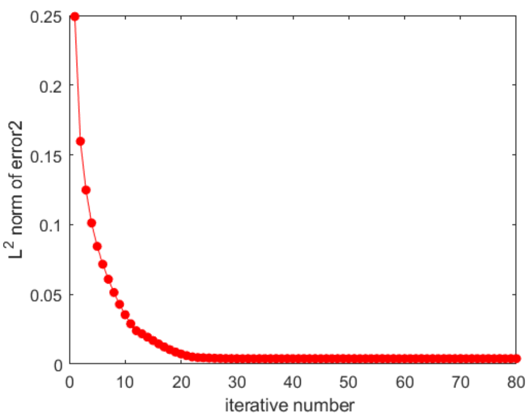

FIGURE 10. Maximum error $\|e_{2k}(\cdot,t)\|_{L^2}$-iteration number curve.

According to the simulation process, we can get the simulation results as shown in Fig. 3 to Fig. 8. Figs. 3-4 represent desired output surfaces $y_{1d}(z,t)$ and $y_{2d}(z,t)$, respectively. Figs. 5-6 represent the actual output surfaces $y_{1k}(z,t)$ (k = 80) and $y_{2k}(z,t)$ (k = 80). By comparing and analyzing Figs. 2-3 and Figs. 5-6, it can be seen that in the 80th iteration, the actual output is consistent with the corresponding expected output profile. In addition, it can be seen from the tracking error surface in space and time shown in Fig. 7 and Fig. 8 that, in the 80th iteration, the maximum tracking error of the surface is 2.049×10^{-3} and 3.889×10^{-3}, respectively.

As the iteration progresses, the iterative learning algorithm becomes more and more effective, as shown in Fig. 9 and Fig. 10. In the 35th iteration, the control performance of the system reaches a better level.

More specifically, the maximum error value of $\|e_{1k}(\cdot,t)\|_{L^2}$ and $\|e_{2k}(\cdot,t)\|_{L^2}$ converge to the specified precision ($<4 \times 10^{-3}$) after the 35th iteration, which confirms the effectiveness of the proposed control algorithm.

V. CONCLUSION

In this paper, an open container motion system with sloshing constraints was transformed into a broader class of SDPS. The ILC is first applied to a linear time-invariant of SDPS. To eliminate the influence of singular terms on the system, the closed-loop D-type ILC algorithm is designed, the convergence theorem of output tracking error is established, and the convergence condition is obtained. Then the correctness of the convergence condition is proved theoretically by rigorous mathematical analysis and proof. In the simulation process, the tracking process of predetermined error accuracy is realized by setting appropriate control parameters, and the actual output completely tracks the expected output with the specified accuracy. Numerical simulation results further verify the effectiveness of the algorithm for the system. Research on SDPS also provides a reference for our further study on the ILC of motion system of open container with sloshing constraints in industrial fluid packaging.

REFERENCES

[1] M. Z. M. Tumari, S. Saat, M. S. Johal, M. F. Bahari, and M. A. Ahmad, "Single input fuzzy logic controller for liquid slosh suppression," *Int. J. Electr. Eng. Appl. Sci.*, vol. 2, no. 1, pp. 45–52, Apr. 2019.

[2] W. J. Yu, Z. H. Zhu, and C. X. Zhong, "Sloshing mode observer and sliding mode attitude control for liquid-filled flexible spacecraft," *J. Nanjing Univ. Sci. Technol.*, vol. 43, no. 5, pp. 640–646, Nov. 2019.

[3] F. Liu, B. Z. Yue, and Y. Tang, "Dynamics modeling and attitude control of spacecraft with multiple propellant tanks," *J. Astronaut.*, vol. 41, no. 1, pp. 19–26, Jan. 2020.

[4] F. Liu, B. Yue, and L. Zhao, "Attitude dynamics and control of spacecraft with a partially filled liquid tank and flexible panels," *Acta Astronautica*, vol. 143, pp. 327–336, Feb. 2018.

[5] H. Peng and G. W. Bao, "Optimal control of liquid slosh on a packaging line," *J. Shanghai Jiaotong Univ.*, vol. 1, pp. 161–164, Jan. 2005.

[6] C. Troll, S. Tietze, and J.-P. Majschak, "Controlling liquid slosh by applying optimal operating-speed-dependent motion profiles," *Robotics*, vol. 9, no. 1, p. 18, Mar. 2020.

[7] B. Nicolsen, L. Wang, and A. Shabana, "Nonlinear finite element analysis of liquid sloshing in complex vehicle motion scenarios," *J. Sound Vibrat.*, vol. 405, pp. 208–233, Sep. 2017.

[8] H. T. Zhang and B. B. Sun, "Analytic calculation of large-amplitude liquid sloshing in tank moving in uniform acceleration motion," *J. Southeast Univ. Natural Sci. Ed.*, vol. 48, no. 2, pp. 207–212, Mar. 2018.

[9] W. Q. Zhao, J. P. Ling, and C. F. Zong, "Development of anti-rollover control strategy for liquid tank semi-trailer," *Automot. Eng.*, vol. 41, no. 1, pp. 50–56, Jan. 2019.

[10] X. J. Song and S. F. Lu, "Attitude maneuver control of liquid-filled spacecraft with unknown inertia and disturbances," *J. Vibrat. Control*, vol. 25, no. 8, pp. 1460–1469, Jan. 2019.

[11] H. Sira-Ramirez, "A flatness based generalized PI control approach to liquid sloshing regulation in a moving container," in *Proc. Amer. Control Conf.*, Jan. 2002, pp. 2909–2914.

[12] B. Bandyopadhyay, P. S. Gandhi, and S. Kurode, "Sliding mode observer based sliding mode controller for slosh-free motion through PID scheme," *IEEE Trans. Ind. Electron.*, vol. 56, no. 9, pp. 3432–3442, Sep. 2009.

[13] S. Kurode, S. K. Spurgeon, B. Bandyopadhyay, and P. S. Gandhi, "Sliding mode control for slosh-free motion using a nonlinear sliding surface," *IEEE/ASME Trans. Mechatronics*, vol. 18, no. 2, pp. 714–724, Apr. 2013.

[14] S. Kurode, B. Bandyopadhyay, and P. S. Gandhi, "Sliding mode control for slosh-free motion of a container using partial feedback linearization," in *Proc. Int. Workshop Variable Struct. Syst.*, Jun. 2008, pp. 367–372.

[15] H. Richter, "Motion control of a container with slosh: Constrained sliding mode approach," *J. Dyn. Syst., Meas., Control*, vol. 132, no. 3, pp. 333–342, May 2010.

[16] K. Yano and K. Terashima, "Robust liquid container transfer control for complete sloshing suppression," *IEEE Trans. Control Syst. Technol.*, vol. 9, no. 3, pp. 483–493, May 2001.

[17] K. Terashima and G. Schmidt, "Motion control of a cart-based container considering suppression of liquid oscillations," in *Proc. IEEE Int. Symp. Ind. Electron. (ISIE)*, Jun. 1994, pp. 275–280.

[18] Q. Zang and J. Huang, "Dynamics and control of three-dimensional slosh in a moving rectangular liquid container undergoing planar excitations," *IEEE Trans. Ind. Electron.*, vol. 62, no. 4, pp. 2309–2318, Apr. 2015.

[19] J. T. Feddema, C. R. Dohrmann, G. G. Parker, R. D. Robinett, V. J. Romero, and D. J. Schmitt, "Control for slosh-free motion of an open container," *IEEE Control Syst.*, vol. 17, no. 1, pp. 29–36, Feb. 1997.

[20] S. J. Chen, B. Hein, and H. Worn, "Using acceleration compensation to reduce liquid surface oscillation during a high speed transfer," in *Proc. IEEE Int. Conf. Robot. Autom.*, Apr. 2007, pp. 2951–2956.

[21] B. Pridgen, K. Bai, and W. Singhose, "Shaping container motion for multimode and robust slosh suppression," *J. Spacecraft Rockets*, vol. 50, no. 2, pp. 440–448, Mar. 2013.

[22] A. Aboel-Hassan, M. Arafa, and A. Nassef, "Design and optimization of input shapers for liquid slosh suppression," *J. Sound Vibrat.*, vol. 320, nos. 1–2, pp. 1–15, Feb. 2009.

[23] N. Sun, Y. Fang, Y. Zhang, and B. Ma, "A novel kinematic coupling-based trajectory planning method for overhead cranes," *IEEE/ASME Trans. Mechatronics*, vol. 17, no. 1, pp. 166–173, Feb. 2012.

[24] N. Sun, Y. Fang, X. Zhang, and Y. Yuan, "Transportation task-oriented trajectory planning for underactuated overhead cranes using geometric analysis," *IET Control Theory Appl.*, vol. 6, no. 10, pp. 1410–1423, 2012.

[25] D. Economou, C. Mavroidis, and I. Antoniadis, "Robust vibration suppression in flexible systems using infinite impulse response digital filters," *J. Guid., Control, Dyn.*, vol. 27, no. 1, pp. 107–117, Jan. 2004.

[26] Z. G. Zhao, L. Liang, and Y. Zhao, "Modified negative input shaping active vibration control," *J. Astronaut.*, vol. 34, no. 10, pp. 1346–1352, Oct. 2013.

[27] M. Grundelius and B. Bernhardsson, "Motion control of open containers with slosh constraints," *IFAC Proc. Volumes*, vol. 32, no. 2, pp. 6142–6147, Jul. 1999.

[28] Y. Zhang, Y. Li, and M. Chen, "Iterative learning control for linear generalized distributed parameter system," *Neural Comput. Appl.*, vol. 31, no. 9, pp. 4503–4512, Nov. 2018.

[29] V. Barbu and A. Favini, "Control of degenerate differential systems," *Control Cybern.*, vol. 28, no. 3, pp. 397–420, 1999.

[30] D. Yue and Y. Q. Liu, "Variable structure control of singular distributed parameter system," *Control Decis.*, vol. 11, no. 2, pp. 278–283, Mar. 1996.

[31] Z. Ge and X. Ge, "Controllability of singular distributed parameter systems in the sense of mild solution," *J. Syst. Sci. Complex.*, vol. 33, no. 5, pp. 1485–1496, May 2020.

[32] Z. Ge, F. Liu, and D. Feng, "Pulse controllability of singular distributed parameter systems," *Sci. China Inf. Sci.*, vol. 62, no. 4, pp. 200–202, Apr. 2019.

[33] X. Dai and X. Zhou, "Mixed PD-type iterative learning control algorithm for a class of parabolic singular distributed parameter systems," *IEEE Access*, vol. 9, pp. 12180–12190, 2021.

[34] Y. Jiang, Q. Zhang, and L. Li, "State feedback control on singular distributed parameter system with parabolic-elliptic type," in *Proc. Chin. Control Decis. Conf. (CCDC)*, May 2016, pp. 261–265.

[35] Y. Jiang and C. Liu, "Explicit spatiotemporal response of singular distributed parameter temperature control system," in *Proc. 36th Chin. Control Conf. (CCC)*, Jul. 2017, pp. 1615–1619.

[36] K. L. Moore, *Iterative Learning Control for Deterministic Systems*. New York, NY, USA: Springer, 1993.

[37] H. S. Ahn, K. L. Moore, and Y. Chen, *Iterative Learning Control: Robustness and Monotonic Convergence for Interval Systems*. Springer, 2007.

[38] M. Wang, Y. Zhang, H. Dong, and J. Yu, "Trajectory tracking control of a bionic robotic fish based on iterative learning," *Sci. China Inf. Sci.*, vol. 63, no. 7, pp. 79–87, May 2020.

[39] Y. Wang, D. Wang, S. Jin, N. Xiao, Y. Li, and E. Frazzoli, "Iterative tuning strategy for setting phase splits with anticipation of traffic demand in urban traffic network," *IET Control Theory Appl.*, vol. 10, no. 12, pp. 1469–1479, Aug. 2016.

[40] L. Strenge, X. Jing, R. Boersma, P. Schultz, F. Hellmann, J. Kurths, J. Raisch, and T. Seel, "Iterative learning control in prosumer-based microgrids with hierarchical control," *IFAC-PapersOnLine*, vol. 53, no. 2, pp. 12251–12258, 2020.

[41] M. B. Delghavi, A. Yazdani, and A. Alizadeh, "Iterative learning control of dispatchable grid-connected distributed energy resources for compensation of grid current harmonic distortions," *Int. J. Electr. Power Energy Syst.*, vol. 131, Oct. 2021, Art. no. 107064.

[42] D. Meng and J. Zhang, "Robust optimization-based iterative learning control for nonlinear systems with nonrepetitive uncertainties," *IEEE/CAA J. Automatica Sinica*, vol. 8, no. 5, pp. 1001–1014, May 2021.

[43] C. Chen, Y. Zhang, Y. Li, Z. Wang, Y. Liu, W. Cao, and X. Wu, "Iterative learning control for a soft exoskeleton with hip and knee joint assistance," *Sensors*, vol. 20, no. 15, p. 4333, Aug. 2020.

[44] R. L. Daugherty and A. C. Ingersoll, *Fluid Mechanics*. New York, NY, USA: McGraw-Hill, 1954.

[45] Y. S. Jiang, "Control design on singular distributed parameter system with parabolic-elliptic type and ecological application," Ph.D. dissertation, College Inf. Sci. Eng., Northeastern Univ., Shenyang, China, 2016.

[46] X. Dai, S. Mei, S. Tian, and L. Yu, "D-type iterative learning control for a class of parabolic partial difference systems," *Trans. Inst. Meas. Control*, vol. 40, no. 10, pp. 3105–3114, Jun. 2018.

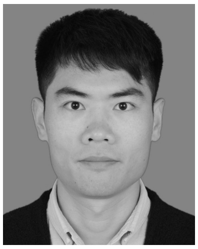

GUANG LI received the B.S. degree in electrical engineering from the College of Engineering and Technology, Hubei University of Technology, Wuhan, China, in 2014, and the M.Sc. degree from Guangxi University of Science and Technology, China, in 2017. In 2017, he joined Guangdong Business and Technology University. He is currently a Lecturer with the School of Information and Automation, Guangdong Polytechnic of Science and Trade. His research interests include iterative learning control and singular distributed parameter systems.

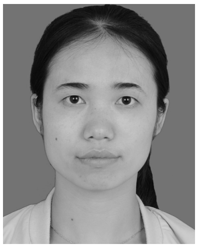

LI HOU received the M.S. degree in control theory and control engineering from Guangxi University of Science and Technology, China, in 2017. In 2017, he joined Guangdong Business and Technology University. He is currently a Lecturer with the School of Mechanical and Electrical Engineering, Guangdong Construction Polytechnic. His research interests include industrial process control and industrial robot systems.

YONG LU received the M.S. degree in control engineering from South China University of Technology, China, in 2012, where he is currently pursuing the Ph.D. degree. In 2019, he joined the School of Information and Automation, Guangdong Polytechnic of Science and Trade, as a Senior Engineer. His research interests include industrial process control and industrial robot systems.